DMD Fast Forward. Published on January 23, 2019 as DOI: 10.1124/dmd.118.085340
This article has not been copyedited and formatted. The final version may differ from this version.

Induction of Cytochrome P450 Involved in the Accelerated Blood Clearance Phenomenon Induced by PEGylated liposomes *in Vivo*

Fengling Wang, Yifan Wu, Jiwen Zhang, Huihui Wang , Xiaoting Xie, Xi Ye, Daiyin Peng, Weidong Chen

Institute of Drug Metabolism, School of Pharmaceutical Sciences, Anhui University of Chinese Medicine, Hefei 230012, Anhui, China (F.W., Y.W., H.W., X.X., X.Y., D.P., W.C.); Department of Pharmacy, The Second People's Hospital of Hefei, Hefei 230011, Anhui, China (F.W., X.Y.); Center for Drug Delivery Systems, Shanghai Institute of Materia Medica, Chinese Academy of Sciences, Shanghai 201203, China (J.Z.)

DMD Fast Forward. Published on January 23, 2019 as DOI: 10.1124/dmd.118.085340
This article has not been copyedited and formatted. The final version may differ from this version.

Running Title Page

CYP450 involved in the ABC phenomenon

Corresponding author: Weidong Chen

Co-corresponding author: Daiyin Peng

Address: School of Pharmaceutical Sciences, Anhui University of Chinese Medicine, Qianjiang 1, Hefei 230012, Anhui, China

Tel: +86-055168129123 E-mail address: wdchen@ahtcm.edu.cn (Weidong Chen) and pengdy@ahtcm.edu.cn (Daiyin Peng)

Fengling Wang and Yifan Wu contribute equally to the manuscript.

Number of text pages: 54

Number of figures: 5

Number of tables: 3

Number of references: 65

Number of words in Abstract: 246

Number of words in the Introduction: 820

Number of words in the Discussion: 1472

Abbreviations

ABC, accelerated blood clearance; AUC, area under the concentration-time curve; AUC_{0-t}, area under the plasma concentration-time curve from time 0 to the last quantifiable time point; $AUC_{0-\infty}$, area under the plasma concentration-time curve from time 0 to infinity; CIM, cimetidine; CLz, plasma clearance; CYP: cytochrome P450; DLS, dynamic light scattering; DSC, differential scanning calorimetry; DTX, docetaxel; HPLC, high performance liquid chromatography; IS,

internal standard; KTZ, ketoconazole; LC-MS/MS, high-pressure liquid chromatography-tandem mass spectrometry; MPS, mononuclear phagocyte system; MRM, multiple reaction monitoring; MRT_{0-t}, mean residence time from time 0 to the last quantifiable time point; $MRT_{0-\infty}$, mean residence time from time 0 to infinity; PBS, phosphate buffered saline; PDI, polydispersity index; PEG, polyethylene glycol; PEG-B-L, blank PEGylated liposomes; PEG-DSPE, distearoyl phosphoethanolamine-PEG_{2000}; PEG-DTX-L, PEGylated liposomal docetaxel; PEG-L, PEGylated liposomes; PTX, paclitaxel; RT-qPCR, real-time quantitative PCR; SD, standard deviation; $t_{1/2}$, half-life; TEM, transmission electron microscopy.

Abstract:

Polyethylene glycol (PEG) is recognized as an attractive excipient to modify liposomes due to their extended-circulation properties. Nevertheless, intravenous injection of PEGylated liposomes (PEG-L) usually trigger a rapid systemic clearance of the subsequent dose from blood circulation that is referred to as "accelerated blood clearance (ABC)" phenomenon. Since the induction of cytochrome P450 (CYP) activity may lead to enhanced drug clearance, it therefore motivated us to investigate the possibility of CYPs involvement in the ABC phenomenon. In this study, PEGylated liposomal docetaxel (PEG-DTX-L) was prepared and used to evaluate the magnitude of the ABC phenomenon in rats induced by repeated injection of PEG-modified liposomes. Notably, ABC phenomenon was observed when the time interval between two doses was from 1 to 7 days, and its magnitude reached the maximum level at 3 days before gradually decreasing. Meanwhile, increased activity of CYP3A1, CYP2C6 and CYP1A2 were detected when PEG-L were repeatedly injected to male rats with a 3 days interval. Consistently, the expression levels of hepatic CYP3A1, CYP2C6 and CYP1A2 were also significantly increased in the repeated injection groups and their levels were highest in the 3-day interval group. CYP selective inhibitors confirmed the inhibition of hepatic CYP3A1 was accompanied by an attenuated magnitude of the ABC phenomenon, which strongly suggests that CYPs may be induced by repeated injection of PEG-L, thus favoring metabolic clearance of the second dose. Collectively, we herein for the first time demonstrate that the contribution of CYPs should not be ignored in the ABC phenomenon.

Keywords: PEGylated liposome; Cytochrome P450; Accelerated blood clearance; Pharmacokinetics; Docetaxel

Introduction

Polyethylene glycol (PEG) is now well-recognized as a vital "stealth" polymer in the drug delivery field, due to its safety, long circulation and non-immunogenicity in humans (Suk et al., 2016). Therefore, PEGylated liposomes (PEG-L) are commonly used as drug delivery vehicles to enhance the therapeutic index of entrapped agents, especially for anticancer drugs, such as Doxil® (Gabizon et al., 2003; Laginha et al., 2005).

Nevertheless, despite the usefulness and excellence of PEGylation, recent reports emphasized that intravenous injection of PEG-L can lead to dramatically reduced half-life ($t_{1/2}$) of the second dose of PEG-L and accumulation in liver and spleen when repeatedly injected *in vivo*. This phenomenon is referred to as the "accelerated blood clearance (ABC)" phenomenon (Dams et al., 2000; Ishida et al., 2005; Ishida et al., 2008). Therefore, ABC phenomenon is a major issue for clinical application of PEG-L that requires multiple injections, as it limits their passive accumulation in many disease sites. The exact mechanism underlying the ABC phenomenon remains unclear.

It is proposed that anti-PEG IgM is produced by spleen cells in response to the first injected PEG-L, which selectively binds to the subsequent dose of PEG-L surface, causing the ABC phenomenon (Ishida et al., 2006b; Ishida et al., 2006c; Shimizu et al., 2015). The magnitude of this phenomenon is influenced by liposomal size, lipid dose, the time interval between two injections, drug encapsulation and animal species (Koide et al., 2012; Yang et al., 2013; Suzuki et al., 2014). Interestingly, the rapid clearance phenomenon has never been reported for Doxil®/Caelyx® and PLD (PEGylated liposomal doxorubicin) (Ishida et al., 2006a; Cui et al., 2008). It is assumed that this kind of liposomes with high cytotoxic drug might be partly taken up

by the spleen, and the drug released from the liposomes inhibits the proliferation of splenic marginal zone B cells and subsequently reduces the secretion of PEG-specific IgM, resulting in failure to induce the ABC phenomenon (Ishida et al., 2006c; Koide et al., 2010). Inconsistently, PEGylated liposomal cytotoxic drug, such as PEGylated liposomal topotecan and epirubicin, could still elicit strong ABC phenomenon (Li et al., 2012; Ma et al., 2012; Li et al., 2013). The contradictory results therefore encourage us to do more detailed research in the ABC phenomenon. Since cytochrome P450 proteins (CYPs) are the major phase I metabolic enzymes involved in oxidative biotransformation of drugs and xenobiotics, and most CYPs predominantly express in the liver (Guengerich, 2008; Burkina et al., 2017). Consequently, the dramatic increase/induction of CYP activity may lead to enhanced clearance and attenuated pharmacological effect as a result of decreased drug plasma levels (Tracy et al., 2016). It is particularly interesting to understand if CYPs are involved in the ABC phenomenon. Seven important CYP isozymes in rats were evaluated in this study, they were CYP1A2, CYP2C6 (homologous to human CYP2C9), CYP2B1 (homologous to human CYP2B6), CYP2C7 (homologous to human CYP2C8), CYP2D2 (homologous to human CYP2D6), CYP2C11 (homologous to human CYP2C19), and CYP3A1/2 (homologous to human CYP3A4/5), which account for a high percentage (~ 70%) of total CYP expression in the liver (Lewis et al., 1998; Lin and Lu, 1998; Lu and Li, 2001; Ingelman-Sundberg, 2004). Probe drugs that are mainly or exclusively metabolized by an individual CYP enzyme can be used to determine the activity of individual CYPs *in vivo*. Recently, relative CYP activity has been determined by quantitative analysis of substrates in a multiple-probe cocktail assay, providing information on the activity of multiple CYP isoforms in a single experiment (Wang et al., 2013; Lee et al., 2015). According to the enzyme selectivity and specificity of probe substrates

and criteria for selecting index substrates recommended by the FDA, we developed a CYP activity cocktail assay using model substrates for the seven important CYPs including CYP1A2 (phenacetin), CYP2B1 (bupropion) (Nishiya et al., 2009), CYP2C7 (amodiaquine), CYP2C11 (omeprazole), CYP2D2 (dextromethorphan) (Walsky and Obach, 2004), CYP2C6 (diclofenac), and CYP3A1/2 (midazolam) (Turpeinen et al., 2009; US FDA, 2017a).

Docetaxel (DTX), a semisynthetic taxane extracted from the needles of the European yew tree (*Taxus baccata*) used for anticancer (Uoto et al., 1997), acted as a model drug for preparing PEGylated liposomal docetaxel (PEG-DTX-L). Notably, ABC phenomenon was caused by the repeated PEG-L in our pilot experiments. It is very interesting to note that the accumulation of DTX in liver was inverse to that in spleen. The greater the magnitude of the ABC phenomenon, the less accumulation of DTX in liver. In this study, we attempted to investigate the effects of the dose of high polymer (PEG-DSPE) and the presence of DTX in the first injection as well as various time intervals between two injections on the ABC phenomenon. Furthermore, we evaluated the issue whether the induction of CYPs is involved in the ABC phenomenon based on CYPs probe cocktail and pharmacokinetics approaches for the evaluation of enzyme activity. In addition, the CYPs mRNA and protein levels were carried out. Finally, specific CYP inhibitors were employed to verify the contribution of CYPs in the systemic clearance of the second PEG-L injection.

Materials and Methods

Materials

DTX (purity>99.0%), paclitaxel (internal standard, purity>99.0%), purified egg yolk lecithin, and cholesteryl hemisuccinate were purchased from Ponsure Biotechnology Co., Ltd. (Shanghai,

China). Distearoyl phosphoethanolamine-PEG_{2000} (PEG-DSPE) was obtained from Shanghai Advanced Vehicle Technology Pharmaceutical Ltd. (Shanghai, China). Analytical grade cholesterol (Chol) and sodium carboxymethyl cellulose (CMC-Na) were purchased from Sinopharm Chemical Reagent Co., Ltd. (Shanghai, China). All lipids were used without further purification. HPLC grade and LC-MS grade acetonitrile and methanol were obtained from Merck (Darmstadt, Germany). LC-MS grade ammonium formate and formic acid were purchased from Fluka Analytical (St. Louis, MO, USA). Docetaxel injection (0.5 mL: 20 mg) was purchased from Jiangsu Heng Rui pharmaceutical Co., Ltd. (Jiangsu, China). High purity (>98.0%) of ketoconazole (KTZ), omeprazole, bupropion hydrochloride, diclofenac sodium, dextromethorphan hydrobromide, amodiaquine hydrochloride, phenacetin and glibenclamide were obtained from National Institutes for Food and Drug Control (Beijing, China). Cimetidine injection (CIM, 0.2 g/2 mL) was from Shangdong Fangming Pharmaceutical Group Co., Ltd. (Shangdong, China). The forward and reverse primers of all target genes were purchased from Sangon Biotech Co., Ltd. (Shanghai, China). TRIzol reagent (Life Technologies Inc., Carlsbad, USA), RevertAid First Strand cDNA Synthesis Kit (Thermo Fisher Scientific, Vilnius, Lithuania) and QuantiNova SYBR Green PCR Kit (QIAGEN, Frankfurt, Germany), Pall nitrocellulose (NC) membrane, 0.22 μm filter (Solarbio Life Sciences, Ltd., Beijing, China) and enhanced chemiluminescence (ECL) reagent kit (Thermo Fisher Scientific, Rockford, USA) were used for detecting mRNA and protein. The antibodies used in this work were mouse anti-CYP3A1, anti-CYP2C6, anti-CYP1A2, anti-GAPDH (Abcam, Cambridge, UK), and anti-mouse HRP-conjugated secondary antibodies (ZSJQ Biotechnology Co., Ltd., Beijing, China). Deionized water was provided by a Milli-Q Reference Ultrapure Water System (Merck, Darmstadt, Germany). All other reagents were

analytical grade.

Preparation of PEG-DTX-L

The optimal formulation of PEG-DTX-L was determined by a single factor analysis and orthogonal test (Gai et al., 2018). PEG-DTX-L, composed of DTX: Chol: Chol hemisuccinate: PEG-DSPE (lipids): lecithin at molar ratios of 1.0: 7.5: 6.6: 4.6: 25.5, were prepared by ethanol injection method as described previously with minor modifications (He et al., 2017). In brief, the lipids and DTX were dissolved in 3 mL absolute ethanol, followed by heating to 50℃. The mixtures were then rapidly injected into 20 mL of stirred (800 rpm) phosphate buffer saline (PBS, pH=7.4). Then suspensions were kept at 50℃ under stirring for 2 hr using an electric stirrer (DF-1 Electric stirrer, Jintan, China). The obtained multilamellar vesicles were passed through a high speed homogenizer (AN GNI AD200L-H, Shanghai, China) for 15 min at 10000 rpm to harvest the small unilamellar PEG-DTX-L. Blank PEGylated liposomes (PEG-B-L) were prepared according to the same procedure as for PEG-DTX-L without adding DTX.

Drug content was assayed in triplicate using a validated high performance liquid chromatography (HPLC, Waters 1525, USA) method as reported earlier (Huang et al., 2013). The HPLC system was equipped with Waters 1525 binary HPLC pump, Waters 2489 UV detector. The stationary phase was performed on a COSMOSIL C_{18} reversed-phase column (4.6 mm×250 mm, 5 μm; Nacalai Lnc, Kyoto, Japan) at 30℃. The mobile phase consisted of acetonitrile: 0.1% phosphoric acid solution (55:45, v/ v) with a flow rate of 1.0 mL/min. The UV detection for DTX was performed at 230 nm. The injection volume was 20 μL and the retention time for DTX was about at 8.60 min. The calibration curve was linear at a range of 0.05 ~ 10 μg/mL with the corresponding linear regression equation of Y = 29518X－835.02 and a correlation coefficient of r=0.9993.

Characterization of PEG-L

Morphological examination. The morphology of the liposomes was carried out using a transmission electron microscopy (TEM, HT7700, JEOL Ltd., Japan). Before observation, the liposome samples were analyzed after 5 times dilution with deionized water to a count rate of 100 ~ 300 kcps, then a drop of PEG-L was plated on a coverslip for about 5 min. After being dried at room temperature, the liposomes were observed by TEM.

Particle size and Zeta potential analysis. Particle size, polydispersity index (PDI) and Zeta potential of the PEG-L were measured by dynamic light scattering (DLS), using Zetasizer size analyzer (Nano ZS90, Malvern Instruments, Malvern, UK) at 25℃. The instrument was calibrated with standard latex liposomes. All measurements of particle size were performed after liposomes were diluted by 20-fold in deionized water. The measurement of Zeta potential for prepared liposomes was performed without dilution. Experimental values were presented from three different results.

Determination of the entrapment efficiency. The DTX encapsulated in the PEG-L was measured indirectly by HPLC method as described previously (He et al., 2017). In brief, the free DTX (non-encapsulated) separated by ultrafiltration/centrifugation technique using Amicon Ultra-4 ultrafiltration centrifuge tube (molecular weight cut off was 100 K, Millipore Corporation, MA, USA). The liposomes properly diluted with deionized water and centrifuged at 3000 rpm for 30 min. The filtrate was obtained and determined by HPLC as free DTX. Drug-loaded liposomes were mixed with methanol for liposomes disruption and dissolved in mobile phase, which was subjected to ultrasound (KQ 300B, Kunshan, China) for 5 min to make drug free from liposomes completely. Then total DTX in liposomes were determined by HPLC after the solution was filtered

through 0.22 μm syringe filter. The drug encapsulation efficiency (EE) was calculated based on the following equation: EE (%) =((W_{total}-W_{free})/ W_{total})×100%, where W_{total}, W_{free} were the weight of total drug in system and weight of free drug in filtrate, respectively. Each experiment was conducted in three independent times.

Differential scanning calorimetry. Differential scanning calorimetry (DSC) experiments were employed to investigate the change of PEG-L crystalline structure using a DSC Q2000 calorimeter (TA Instrument, USA). Hermetically aluminum sealed pan was filled with approximately 5 mg of sample, while an empty pan was used as the reference. The data of DTX, Chol, Chol hemisuccinate, PEG-DSPE, lecithin, their physical mixture, lyophilized PEG-DTX-L and PEG-B-L were recorded at a scan rate of 10℃/min from 20℃ to 200℃.

In vitro release kinetics. The dialysis bag diffusion technique was used to study the *in vitro* drug release of DTX from the PEG-L according to a procedure similar to that described by He *et al*. (2017). Briefly, PEG-L dispersion equivalent to 0.5 mg of drug was filled into a dialysis membrane bag (21 mm, MVCO8000-14400 Da, USA), hermetically sealed and immersed into a beaker containing 100 mL of PBS (pH 7.4) containing 0.1% w/v Tween-80. The entire system was kept at (37 ± 0.5) ℃ with continuous stirring at 100 rpm. Samples were taken out from the beaker at predetermined time intervals and replaced by fresh medium to maintain the sink condition. The amount of DTX released from PEG-L were analyzed by HPLC as described above (Determination of the entrapment efficiency). Cumulative percentage release was then calculated from the amount of drug release. Each releasing experiment was carried out in triplicate.

Experimental animals and ethics statement

Male Sprague-Dawley (SD) rats, five-week-old (220 ± 15 g) were obtained from the Experimental

Animal Center of Anhui Medical University (Hefei, China). The experimental animals were allowed free access to water and a commercial rodent diet. They adapted to the controlled experimental conditions of 25 ± 2 ℃, humidity 60 ± 5% with a 12 hr light/dark cycle for 1 week before experiments. All the procedures involving experimental animals were carried out in accordance with the guidelines evaluated and approved by Institutional Animal Care and Use Committee, Anhui University of Chinese Medicine.

Pharmacokinetics and biodistribution of PEG-L after repeated administration

Injection Protocols. Male SD rats were randomly and equally divided into 5 groups for pharmacokinetics and biodistribution investigations according to completely randomized digital table, and formulations were injected intravenously via tail vein (n=6 for each group). PEG-DTX-L and PEG-B-L were freshly prepared before administration. For the purpose of comparison the effect of different time intervals on the magnitude of the ABC phenomenon, PEG-DTX-L was injected into animals after the first injection of PEG-B-L for 1, 3, 5 or 7 days. Rats in group 1 d, 3 d, 5 d and 7 d all received two doses, PEG-B-L (containing 0.05 μmoL of PEG-DSPE/kg) on day 0 and then 2.5 mg/kg PEG-DTX-L after 1, 3, 5 or 7 days. Rats in group 0 d were only treated with a single injection of 2.50 mg/kg PEG-DTX-L, which was used as a control. Here, the dose of PEG-DTX-L represented the amount of drug not phospholipid. The detailed injection protocols for PEG-DTX-L and PEG-B-L are presented in Table 1.

Sample preparation. About 0.3 mL orbital venous blood samples were collected under isoflurane anesthesia into sodium heparin tubes immediately prior to (blank sample) and following the predetermined post-injection time points (0.167, 0.5, 1, 2, 4, 6, 8, 10, and 12 hr). Plasma samples were centrifuged at 3000 rpm for 10 min, and subsequently plasma (100 μL) was obtained and

stored at -80℃ until further liquid chromatography-tandem mass spectrometry (LC-MS/MS) analysis.

Rats were euthanized with isoflurane anesthesia after the last blood sample was harvested at 12 hr, and tissues of interest (liver and spleen) were collected and flash frozen in liquid nitrogen and stored at -80℃. Upon processing, tissues were thawed and diluted in a 1: 2 ratio (w/v) with PBS (pH 7.4) prior to homogenizing with a T18 digital ULTRA-TURRAX® homogenizer (IKA® Works Guangzhou, Guangzhou, China). Plasma or tissue homogenate was further processed by 3-fold of methyl tert-butyl ether with 250 ng/mL paclitaxel (internal standard, IS) and swirled for 5 min. After centrifuged at 12,000 rpm for 5 min at 4℃, the supernatant was removed to a clean tube, evaporated to dryness under nitrogen, and reconstituted in 100 μL of methanol. The samples were then swirled, transferred to autosampler vials, and analyzed by LC-MS/MS.

LC–MS/MS conditions. The chromatographic system consisted of a G6460H MS/MS spectrometer (Agilent Technologies Inc., Waldbronn, Germany) coupled to an Agilent 1260 series HPLC system (Agilent Technologies Inc., Shanghai, China). Chromatographic separations were carried out using a DIKMA® Leapsil C_{18} column (3.0 mm×50 mm, 2.7 μm), maintained at 30℃.

The LC mobile phase consisted of water containing 1 mM ammonium formate, acidified to pH 6.5 with formic acid (solvent A) and methanol (solvent B) in a 27: 73 ratio (v/v) with a flow rate of 0.4 mL/min and an injection volume of 5 μL. The overall run time was 4.0 min. The mass spectrometer was operated in the positive electrospray ionization mode (ESI^+). The detection was operated in the multiple reaction monitoring (MRM) mode. The optimized MRM transitions were m/z 830.4→549.3 with a fragment voltage of 135 V and a collision energy of 15 V for DTX and m/z 876.8→308.5 with a fragment voltage of 115 V and a collision energy of 18 V for paclitaxel

(IS), respectively. Representative parent ion and product ion spectrum of DTX and IS are given in Supplemental Figure 1. Typical chromatograms of DTX and IS showed no interfering peak in the blank matrices was observed under these experimental conditions (Supplemental Figure 2).

Method validation. The LC-MS/MS methods for analysis plasma and tissue samples were linear in the concentration range of 2.5 ~ 2000 ng/mL (r=0.999) and 5 ~ 1000 ng/mL (r=0.995), respectively. Calibration curves were established by employing a linear regression with a weighting factor of $1/x^2$. The lowest limit of quantifications (LLOQ) for plasma and tissue samples estimated at signal to noise ratio near or above 10, were 2.5 ng/mL and 5 ng/mL respectively. For intra- and inter-assay accuracy performance was assessed by analyzing five replicates of samples at four-level quality control [LLOQ, low quality control (LQC), middle quality control (MQC) and high quality control (HQC)] concentrations on three consecutive days, the median recoveries for intra- and inter-assay of DTX were ranged from 98.4% to 107.6% in plasma, 99.6% to 104.8% in liver, and 99.9% to 113.6% in spleen. The coefficient of variations (CVs) of intra- and inter-assay of DTX in plasma, liver and spleen samples were ranged from 5.2% to 17.5%, 4.4% to 17.9%, and 3.7 to 14.2%, respectively (Supplemental Table 2). The stabilities of DTX in plasma, liver and spleen were evaluated at the LQC and HQC levels with six replicates under different conditions, including stock solution, autosampler, short-term, long-term, and freeze-thaw stability (Supplemental Table 3). The results demonstrated five types of stability were within acceptance criteria. Six different lots of blank plasma were used to assess the extraction efficiencies and matrix effects at three QC levels. The extraction recovery of DTX, as determined in six replicates, was about 78.6 ~ 89.4% in plasma, 82.0 ~ 96.8% in liver, and 90.3 ~ 99.1% in spleen. The CVs for three levels were all less than 10%. IS-normalized matrix factor

(MF) was recommended as a marker to evaluate matrix effect (Bansal and DeStefano, 2007). The MFs of DTX in plasma and tissue varied from 92.7% to 107.9%, with CV values less than 15.0% (Supplemental Table 4). No significant interference in the blank matrices was observed from other endogenous substances in this method, indicating feasible sample preparation. These results all met the acceptance criteria of FDA guideline for bioanalytical method validation (US FDA, 2018), suggested that the developed method could be applied for the pharmacokinetic study of DTX. A non-compartment model was used to calculate the pharmacokinetic parameters of different animal groups after repeated injection of PEG-L using DAS 2.0 software (Shanghai Bojia Medical Technology co., Ltd, Shanghai, China).

Determination of CYP activity by the LC-MS/MS

Experimental design. Male SD rats were randomly divided into 5 groups (n=8 per group). Both PEG-L and CYPs probe cocktail solution were freshly prepared before administration. For the purpose of comparison the effect of the single and repeated injection of PEG-L (with a 3-day interval) on CYP activity, all animals received intravenous injection of probe cocktail solution, containing phenacetin (0.4 mg/kg), bupropion (0.4 mg/kg), amodiaquine (1.2 mg/kg), omeprazole (0.4 mg/kg), dextromethorphan (0.4 mg/kg), diclofenac (0.4 mg/kg), and midazolam (0.4 mg/kg) dissolved in physiological saline (containing 3% absolute ethanol) after single or repeated PEG-L injection for 30 min, which used as single PEG-L injection group and repeated PEG-L injection group. In order to exclude the influence from DTX itself (the burst release of DTX in the initial time from the surface or encapsulated in the outermost layers), the same dose of DTX injection was injected into animals with a single injection or repeated injections (with 3 days interval) before the treatment of probe cocktail solution, which used as single DTX injection

group and repeated DTX injection group. The detailed PEG-L/CYP probe-drug administration was described in Table 2. Control rats were injected with the same volume of PBS as the two doses.

Blood sample preparation. Blood samples (0.3 mL) were collected from the orbital venous under isoflurane anesthesia into heparinized 1.5 mL of polythene tubes immediately prior to (blank sample) and following the predetermined time points (3, 10, 30, 45, 60, 90, 120, 240, and 360 min) after injection of probe cocktail solution. Plasma samples were immediately centrifuged at 3000 rpm for 10 min. Subsequently, plasma (100 μL) was obtained and stored at -80 ℃ until further LC-MS/MS analysis.

LC–MS/MS conditions. The chromatographic system is the same as mentioned above. The LC mobile phase consisted of water containing 0.1% formic acid (solvent A) and acetonitrile (solvent B). The binary solvent gradient elution (0.2 mL/min flow rate) was optimized as follows: 10% B at the time of injection, a linear increase to 80% B to 1 min, remaining at 80% B to 1.3 min, an increase to 95% B to 2 min, a decrease to 90% B to 3 min, remaining at 90% B to 3.5 min, and then decrease to 10% B to 5 min, and maintained at 10% B for additional 3 min for re-equilibration.

Quantitation was performed by MRM in the positive ESI^+ mode and the related product ion for each probe drug. The optimized MRM transitions, fragment voltages and collision energies determined for each probe drug and IS are listed in Supplemental Table 7. The typical chromatographs (Supplemental Figure 3) indicate that the response of endogenous compounds had no significant influence on determining the probe drugs in the current conditions.

Method validation. To evaluate the sensitivity, reliability and specificity of the LC-MS/MS method, the LLOQ, linearity of standard curve, accuracy, precision stability, extraction efficiency

and matrix effect for each probe drug were validated. As shown in Supplemental Figure 3 and Supplemental Table 9 ~ 11, all results of selectivity, sensitivity, linearity, accuracy, precision, stability, extraction efficiency as well as matrix effect met the requirement in the FDA bioanalytical method validation guidance (the detailed results were described in Supplemental Result 2 (Baghdasaryan et al., 2014), indicate that the developed method could be applied to determine the levels of all probe drugs in rat plasma. DAS 2.0 software was used to estimate pharmacokinetic parameters calculated by a non-compartment model, parameters of the seven substrates were used to represent relative activity of the seven isozymes.

Real-time quantitative PCR (RT-qPCR)

Total RNA isolation and cDNA synthesis as well as RT-qPCR were performed as described previously (Rio et al., 2010; Doak and Za ř, 2012; Roth et al., 2018). Briefly, total RNA was extracted from tissue samples using TRIzol reagent following the manufacturer's protocol. RNA concentration and purified were determined spectrophotometrically using a SoftMax® Pro 5 Multiscan Spectrum (Molecular Devices, Silicon Valley, USA) with the OD_{260} nm/OD_{280} nm ratio expected to be 1.8 ~ 2.0. Total RNA (5 μg) extracted from each tissue was reverse-transcribed using RevertAid First Strand cDNA Synthesis Kit, according to the manufacturer's instructions. Subsequently, all cDNA samples were diluted 30 times and stored at 80℃ until use. For the assessment of RNA expression, cDNA was amplified using a StepOne Plus PCR System (Applied Biosystems, CA, USA) with SYBR Green PCR kit, and the forward and reverse primers (details of the primer sequences used are given in Supplemental Table 12). The cycling parameters were performed as follows: one cycle of initial denaturation (95℃, 10 min), followed by quantification with 40 cycles of denaturation (95℃, 15 s) and annealing (60℃, 60 s). Finally, specificity of

target amplification confirmed by an additional cycle (95 ℃ for 15 s, 60 ℃ for 60 s, and 95 ℃ for 15 s). For all calculations regarding qPCR, the comparative CT ($2^{-\Delta\Delta CT}$) method was applied to determine the relative mRNA expression using β-actin as an endogenous reference gene. Each RT-qPCR reaction was performed in triplicate.

Western blotting

For protein analysis, about 50 mg liver tissue was homogenized and lysed in 1 mL RIPA lysis buffer for 30 min on ice. Total protein concentration was quantified by BCA protein assay method. Subsequently, the lysates were diluted in 5×SDS-PAGE loading buffer containing 5% β-mercaptoethanol, denatured by boiling 10 min at 95℃ and protein samples (20 μg) were separated by 12% SDS-PAGE. After proteins were transferred to NC membrane using wet blotting on ice (200 mA, 2 hr) and blocked with 5% skimmed milk in Tris buffered saline containing 0.05% Tween-20 (TBST) at room temperature for 2 hr, the membranes were then incubated with an appropriate dilution of the primary antibody at 4 ℃ overnight. After washing with TBST, the membranes were incubated the appropriate HRP-conjugated secondary antibody in blocking solution at room temperature for 1 ~ 2 hr. Finally, the bands were detected by using the ECL detection kit according to the manufacturer's instructions and expression levels were normalized to GAPDH. The determination of all protein expression was performed in triplicate and the results were reproducible. Autoradiographs were scanned using Alpha Chemiluminescent gel imaging system FluorChem FC3 (ProteinSimple, silicon valley, USA) and quantified using the ImageJ software (version 1.45S, NIH, USA).

Inhibition study of the ABC phenomenon in vivo

In order to verify the role of CYP enzymes in the process of PEGylated liposome-induced ABC

phenomenon, the relatively selective CYP inhibitors were used in this study, including ketoconazole (KTZ, strong inhibitor of CYP3A1 as well as weak inhibitor of CYP1A2 and CYP2C6 in rats) and cimetidine (CIM, strong inhibitor of CYP2C6 and weak inhibitor of CYP1A2 in rats) reference to the recommended guidance by the US FDA (2017b) and previous reports (Meredith et al., 1985; Mosca et al., 1985; Levine et al., 1998; Kotegawa et al., 2002; Yang et al., 2018). The inhibition study consisted of six groups (n=6 for each group). The rats were administered the following treatments: (1) To inhibit CYP3A1, rats in group 1 were pretreated with oral administration of KTZ (suspended in 0.5% CMC-Na, 100 mg/kg/day) for 7 days + treated with the first injection of PEG-B-L at the 4th day and the repeated injection of PEG-DTX-L (2.5 mg/kg) at the 7th day (3 d KTZ+); (2) Rats in group 2 were pretreated with an equal volume of 0.5% CMC-Na for 7 days + treated with the first injection of PEG-B-L at the 4th day and the repeated injection of PEG-DTX-L (2.5 mg/kg) at the 7th day (3 d KTZ-); (3) Rats in group 3 were pretreated with an equal volume of 0.5% CMC-Na for 7 days followed by a single injection of 2.5 mg/kg PEG-DTX-L (Control). (4) To inhibit CYP2C6, rats in group 4 received the first injection of PEG-B-L at the 1st day, and 3 days later, rats were pretreated with a single intraperitoneal dose (150 mg/kg, dissolved in 0.9% saline) of CIM for 1.5 hr before the second dose of 2.5 mg/kg PEG-DTX-L (3 d CIM+); (5) Rats in group 5 received the first injection of PEG-B-L at the 1st day, and 3 days later, rats were pretreated with an equal volume of 0.9% saline for 1.5 hr before the repeated injection of 2.5 mg/kg PEG-DTX-L (3 d CIM-); (6) Rats in group 6 were pretreated with an equal volume of 0.9% saline for 1.5 hr followed by a single injection of 2.5 mg/kg PEG-DTX-L (Control). Here, PEG-B-L in all groups is the same (containing 0.05 μmol of PEG-DSPE/kg). The preparation and detection conditions in LC-MS/MS for blood and tissue

samples were the same as mentioned above.

Statistical analysis

All data subjected to statistical analysis was obtained from at least three parallel experiments, data are expressed as mean ± standard deviations (SD). Each set of results was first evaluated for normal distribution using Kolmogorov-Smirnov test. Normally distributed data of multiple comparison was analyzed by one-way ANOVA followed by a Student-Newman-Keuls post-hoc test for statistical comparisons of two groups (IBM SPSS 23.0 software, IBM Corporation, Armonk, NY). In Supplemental Table 15 ~ 17, the differences in pharmacokinetic parameters were examined using nonparametric test (Kruskal-Wallis) followed by Dunn's test. The level of significance was set at $p < 0.05$, $p < 0.001$. The pharmacokinetic parameters were calculated by non-compartment model analysis using DAS 2.0 software package (Shanghai Bojia Medical Technology co., LTD, Shanghai, China).

Results

Characterization of PEG-L

Particle size, polydispersity, Zeta potential, EE, and morphology analysis. Generally, the physiochemical properties of the colloidal systems including the mean particle size, polydispersity index (PDI) and Zeta potential are strongly associated with their performance and biological activity. As shown in Supplemental Table 13 and Supplemental Figure 4, the mean particle sizes of before loading and after loading were similar (about 110 nm), owing to the presence of PEG on the surface of the liposomal carrier resulting in the formation of steric hindrance on the liposome surface (Immordino et al., 2006). Moreover, the formulation had a narrow size distribution, with a PDI value ranging from 0.127 to 0.173, indicating the PEG-L dispersed uniformly. The analysis of

Zeta potential is a critical parameter to predict the physical storage of delivery systems. Higher absolute value of Zeta potential indicated greater repulsion between particles, and the aggregation is less likely to occur. In this study, all liposomes were negatively charged (-27.0 ± 0.35 mV for PEG-B-L, -32.40 ± 1.04 mV for PEG-DTX-L) due to the presence of PEG-DSPE on the surface. As shown in TEM image (Supplemental Figure 5), liposomes display uniform diameters in the nanometer scale and disperse homogeneously with regular spherical shape, which is consistent with the DLS results. In addition, this formulation displayed a high EE value of (96.62 ± 0.95) % and no aggregation was found among the particles.

DSC study. DSC studies were performed to investigate the phase transition temperature of PEG-DTX-L formulation along with its individual components. Each melting temperature (T_m) is different when comparing the sharp peaks in Supplemental Figure 6. The DSC thermogram of raw material DTX was a wide peak at 163.33℃ (curve B), and relatively sharp peaks at 150.04 ℃, 55.09 ℃, 125.86 ℃, and 185.75 ℃ were respectively obtained from the Chol, PEG-DSPE, lecithin, chol hemisuccinate (curve E, F, G, and H). The T_m of the physical mixture was near 51.04 ℃ (curve D), which was the lowest T_m in the DSC thermograms. The incorporation of DTX in the liposomes formulation had increased the T_m of PEG-B-L by 3.7℃ and affected the transition phase behavior as detected by DSC. This confirms the incorporation of DTX and other materials lead to the change of liposomes crystalline structure.

In vitro release kinetics of PEG-DTX-L. In general, the release rate of drug is important in colloidal delivery systems, which is associated with the *in vivo* performance. In order to evaluate the controlled release potential of PEG-DTX-L, release profiles of free DTX and DTX from PEG-L were investigated up to 36 hr (Supplemental Figure 7). As expected, more than 80% of

free DTX was measured in the initial 2 hr. Obviously, the dissolution and diffusion rate of PEG-DTX-L was much slower than free DTX solution. Release dosing in the initial 0.5 hr was nearly 30.2%, which may be attributed to the adsorbed drug on the surface or encapsulated in the outermost layers of the liposomes, followed by a slow and sustained profile, reaching approximately a 46.2% of released drug after 36 hr. Therefore, the accumulative release profiles demonstrate that the lipid bilayer can change the rate of dissolution and diffusion of DTX under the described experimental conditions. The obtained release kinetic model of free DTX and PEG-DTX-L both fitted well with First-order kinetics: ln(1-Q)=-0.2401t-0.9888, r=0.8478 and ln(1-Q)=-0.2702t-0.7427, *r*=0.8485, respectively.

Effect of PEG-L with time intervals on the induction of the ABC phenomenon upon repeated injection

As revealed by our study (the detailed results are described in Supplemental Result 1), the initial injection of PEG-B-L triggered an apparent ABC phenomenon that significantly accelerated the blood clearance rate of subsequently injected liposomes, which was comparable with that of DTX encapsulated in liposomes (Supplemental Figure 8 and Supplemental Table 5 ~ 6), suggesting the liposomes induced the ABC phenomenon and not DTX. The results are consistent with those of previous studies performed for liposomes (Ma et al., 2012), indicating that PEG-L can induce ABC phenomenon by themselves after repeated injection and the addition of DTX in PEG-L did not alter what was seen with the blank formulation. Moreover, PEG-DSPE content of the liposomes that were initially injected did not affect the extent of the ABC phenomenon within the range of 0.025 ~ 0.05 μmoL/kg of PEG-B-L in this study (Supplemental Figure 8 and Supplemental Table 5 ~ 6), which is in agreement with those reported by Ishihara and co-workers

(Ishihara et al., 2009) who reported that the extent of the ABC phenomenon was not apparently changed with the increased dose of PEG polymer in the initial dose. It was also confirmed that a specific range of PEG polymer pre-dose do not affect ABC induction, but that a larger proportion of PEG polymer inhibited the ABC phenomenon (Saadati et al., 2013).

The issue of whether the time interval between two injections has influence on the induction of the enhanced clearance effect was assessed via comparing the pharmacokinetics and biodistribution behavior upon repeated injections. Rats in five groups (1 d, 3 d, 5 d and 7 d) were injected with two injections of PEG-L at various time intervals (1 day, 3 days, 5 days and 7 days, respectively) between the initial and the second dose. The ABC phenomenon was evaluated by examining area under the concentration-time curve (AUC) and $t_{1/2}$ of the experimental payload (DTX). $AUC_{C/T}$ (ratio of AUC of the control group to the test group) and $t_{1/2C/T}$ (ratio of $t_{1/2}$ of the control group to the test group) were previously used as major markers to assess the altered pharmacokinetic profiles of these groups (Xu et al., 2015). The results shown in Supplemental Table 14 and Figure 1A are similar to those reported in previous studies (Ishida et al., 2006a; Cui et al., 2008), the pharmacokinetic profiles of the four test groups were dramatically different compared with the single dose control. The ABC phenomenon occurred after repeated injection of PEG-DTX-L at different time intervals (1 day, 3 days, 5 days, and 7 days). The values of area under the plasma concentration-time curve from 0 to the last quantifiable time point (AUC_{0-t}) and mean residence time from time 0 to the last quantifiable time point (MRT_{0-t}) in the test groups (1 d, 3 d, 5 d and 7 d) were significantly decreased compared to control (0 d). Particularly for group 3 d, the value of plasma clearance (CLz) (0.74 ± 0.16 L/hr/kg) was significantly higher ($p < 0.01$) and the values of AUC_{0-t}, MRT_{0-t} and $t_{1/2}$ (3053.35 ± 587.38 μg/L·hr, 3.84 ± 0.31 hr and 4.09 ± 1.05 hr, respectively)

were distinctly lower (p<0.05) than those of the control. Thus, the magnitude of the ABC phenomenon reached the maximum level on three days after the initial dose. In group 5 d and 7 d, the CLz value of PEG-DTX-L (0.50 ± 0.16 L/hr/kg and 0.33 ± 0.12 L/hr/kg, respectively) was less than that of group 3 d. With the decrease in the *in vivo* clearance, the AUC_{0-t}, mean residence time from time 0 to the last quantifiable time point (MRT_{0-t}) and $t_{1/2}$ values of group 5 d and 7 d were higher than those of group 3 d (Supplemental Table 14). Therefore, the magnitude was gradually decreased as the time interval between doses extended from 3 days to 7 days (Table 3). Therefore, repeated injection of PEG-L with a time interval of 3 days could induce the strongest ABC phenomenon, and the prolongation of time interval between two injections alleviated the magnitude of the ABC phenomenon, which is consistent with previous reports (Li et al., 2013). Nevertheless, the enhanced accumulations of the second dose in liver and spleen were apparently different among the liposome treated groups (Figure 1B). The control rats exhibited very low accumulations of DTX in liver and spleen. Compared to the control group, the lowest concentration of DTX accumulated in the liver of group 3 d at 12 hr with an obvious ABC effect, while the accumulation of DTX in spleen was far higher than that of the control and other test groups. Interestingly, with the prolonged time interval, increased accumulation of the second dose in liver and decreased accumulation in spleen were observed. Inconsistently, compared with the results in Figure 1B, the relative liver accumulation of DTX in group 3 d increased by nearly 3-fold at 4 hr after the second dose (Data not shown), while no significant changes was found in the spleen accumulation. Together, these data imply that pretreatment with PEG-L trigger a rapid accumulation of the second dose in liver at the initial time, followed by a remarkable reduction of hepatic DTX in the later hours. We hypothesized that the accelerated metabolism of

the drug was caused by CYP enzymes, as it is known that hepatic CYPs play essential role in the process of drug metabolism, which might be induced by repeated injection of PEG-L. It is therefore particularly interesting to understand whether the activation of CYPs is involved in the ABC phenomenon.

The activity and expression of CYPs in plasma induced by single injection or repeated injection of PEG-L

Determination of CYP activity. In this study, the issue of whether repeated injection of PEG-L lead to the activation of CYPs was investigated. A marked difference of pharmacokinetic profiles of several probes was observed between single PEG-L injection group and repeated PEG-L injection groups using a probe cocktail assay in rats (Figure 2 and Supplemental Table 15~17). For midazolam (probe for CYP3A1/2 in Supplemental Table 15), the CLz value for the repeated PEG-L injection group (0.24 ± 0.07 L/hr/kg) was increased significantly ($P < 0.01$), compared with those of the single PEG-L injection group (0.12 ± 0.02 L/hr/kg). Along with the increase in the *in vivo* clearance, the AUC_{0-t} and area under the plasma concentration-time curve from time 0 to infinity ($AUC_{0-\infty}$) values for the repeated PEG-L injection group (4455.52 ± 1511.12 μg/L·hr and 4494.27 ± 1517.96 μg/L·hr, respectively) were significantly decreased ($P < 0.01$), compared with those of the single PEG-L injection group (7989.68 ± 1456.23 μg/L·hr and 8266.47 ± 1490.49 μg/L·hr, respectively). In addition, the $t_{1/2}$ value for the repeated PEG-L injection group was also decreased compared to that of the single PEG-L injection group ($P < 0.05$). For diclofenac (probe for CYP2C6) in Supplemental Table 16, the CLz value for the repeated PEG-L injection group (1.20 ± 0.48 L/hr/kg) was increased significantly ($P < 0.01$) compared with those of the single PEG-L injection group (0.26 ± 0.09 L/hr/kg). Similar to midazolam, corresponded

with decrease in AUC_{0-t} and $AUC_{0-\infty}$ after repeated PEG-L injection (846.69 ± 294.10 μg/L·hr and 937.18 ± 297.09 μg/L·hr, respectively) compared with those of the single PEG-L injection group (2734.07 ± 413.23 μg/L·hr and 4517.64 ± 2426.29 μg/L·hr, respectively) ($P < 0.01$). In addition, the $t_{1/2}$, MRT_{0-t} and mean residence time from time 0 to infinity ($MRT_{0-\infty}$) of the repeated PEG-L injection group were also decreased compared to those of the single PEG-L injection group ($P < 0.01$). For the CYP1A2 probe phenacetin (Supplemental Table 17), the CLz value for the repeated PEG-L injection group (7.24 ± 2.87 L/hr/kg) was increased significantly ($P < 0.01$) compared with those of the single PEG-L injection group (3.71 ± 1.38 L/hr/kg), and the AUC_{0-t} and $AUC_{0-\infty}$ values for the repeated PEG-L injection group were decreased significantly ($P < 0.01$). In addition, the $t_{1/2}$ of the repeated PEG-L injection group was decreased compared to that of the single PEG-L injection group but not reached significant difference. Taken together, these results indicate that the pharmacokinetics of CYP3A1, CYP2C6 and CYP1A2 probe substrates are altered apparently by repeated injection of PEG-L. No significant difference was detected in the pharmacokinetic characteristics of CYP2B1 probe bupropion, CYP2C7 probe amodiaquine, CYP2C11 probe omeprazole and CYP2D2 probe dextromethorphan (data not shown). The pharmacokinetic characteristics of the three probes (midazolam, diclofenac and phenacetin) were not altered with repeated DTX injections (Supplemental Figure 9), indicating the CYP response is not due to the burst release of DTX from PEG-L.

Determination the expression of CYPs mRNA and protein. Gene transcription and protein expression of CYP3A1, CYP2C6 and CYP1A2 upon repeated injection at different time intervals were evaluated. The expression of hepatic CYPs mRNA and protein levels in five groups that received PEG-DTX-L after dosing of PEG-B-L for 0, 1, 3, 5 and 7 days (0 d, 1 d, 3 d, 5 d and 7 d)

were determined. In order to compare the change of CYPs expression profiles clearly, normal control (NC) rats received a single injection of equivalent volume PBS. As shown in Figure 3A, significant increase in mRNA expression of CYP3A1, CYP2C6 and CYP1A2 were observed in the test groups when compared to control rats. Consistently, the protein expression levels of CYP3A1, CYP2C6 and CYP1A2 were also found to be upregulated in the test groups compared with the control group (Figure 3B). Concerning CYP3A1 expression, significant increase of mRNA expression were detected in group 1 d, 3 d and 5 d with apparent increase of protein level in group 3 d and 5 d. Increased CYP2C6 mRNA and protein levels were found in group 3 d, 5 d and 7 d. CYP1A2 mRNA level were increased in group 3 d and 5 d and protein levels were elevated in group 3 d, 5 d and 7 d. Hence, these data suggest that liver CYP activity differences might be partly, but not absolutely, owing to the differences in their mRNA and protein expression. It is worth mentioning that the mRNA and protein expression of the three CYP isoforms increased from group 1 d and reached a peak in group 3 d before gradually decreasing with extended time interval, which is in accordance with the result of the ABC magnitude observed in the pharmacokinetic experiments. Meanwhile, the relative concentration of DTX accumulated in liver of group 3 d fell to the lowest point after the reinjected dose for 12 hr. This suggests CYPs might be responsible for the rapid clearance of the second dose in plasma and liver.

Effects of the presence of CYP inhibitors on ABC phenomenon

The effects of selective CYP inhibitors on PEG-DTX-L metabolism were investigated by pretreating with vehicle or selective CYP inhibitors before administration of repeated PEG-L injection with a time interval of 3 days (Figure 4 and Supplemental Table 18). In comparison with group 3 d (KTZ-), the value of $t_{1/2C/T}$ for group 3 d (KTZ+) was reduced by 1.88 times whereas the

DMD Fast Forward. Published on January 23, 2019 as DOI: 10.1124/dmd.118.085340
This article has not been copyedited and formatted. The final version may differ from this version.

value of $AUC_{C/T}$ was not decreased apparently. It was worth mentioning that KTZ inhibited the depletion of DTX in the liver. The accumulation of DTX in liver was upregulated dramatically ($P < 0.01$) in group 3 d (KTZ+) compared to group 3 d (KTZ-), while a comparable results of spleen was found in the two test groups (Figure 4B). As for CIM, neither $AUC_{C/T}$ nor $t_{1/2C/T}$ were significantly decreased in group 3 d (CIM+) when compared with group 3 d (CIM-) (Figure 4C and Supplemental Table 18). Likewise, the accumulations of DTX in liver and spleen was not changed with CIM inhibition (Figure 4D). These results revealed that pretreated with KTZ attenuated the ABC magnitude in a small degree.

In addition, the inhibition of KTZ and CIM on hepatic CYPs expression was assessed. Pretreatment with KTZ revealed that the mRNA and protein expression of CYP3A1 and CYP1A2 were apparently down-regulated compared with those of group 3 d (KTZ-), while no significant difference was observed for the expression of CYP2C6 (Figure 5A and B). The significantly down-regulated mRNA and protein expression of CYP2C6 and CYP1A2 were found in group 3 d (CIM+) in comparison with group 3 d (CIM-), while no significant difference was observed for the expression of CYP3A1 (Figure 5 C and D). For the probe substrate DTX, CYP3A (CYP3A4/5 in humans and CYP3A1/2 in rats) may play a more significant role for substrate, where these enzymes are responsible for the metabolism of the selected probe (Vaclavikova et al., 2004). Therefore, these findings suggest that the significant increased CYPs (especially for CYP3A1) induced by repeated injection of PEG-L are involved in the induction of the ABC phenomenon, whereas CYP2C6 and CYP1A2 play negligible or minor roles.

Discussion

Despite the superior merits and usefulness of PEGylation in liposome-based therapeutics,

increasing evidence suggests that the injection of PEG-L into different species of animals can trigger ABC phenomenon, which is an urgent and serious problem to be overcome for the clinical use of liposome-based drug delivery systems (Li et al., 2012; Li et al., 2013; Suzuki et al., 2014). Previous reports have revealed that the time interval between injections considerably affect the magnitude of the ABC phenomenon (Ishida et al., 2003; Li et al., 2013). Dams et al. (2000) had first shown that pre-injection with PEG-L in rats and a rhesus monkey for 7 days induced the rapid clearance and enhanced the accumulations of the second injection of PEG-L in liver and spleen, and the extent of this phenomenon was most apparent at a time interval of 6 ~ 7 days. Later on, a series of findings confirmed the optimal time interval for the most effective induction of the ABC phenomenon is from 3 to 10 days (Li et al., 2012; Saadati et al., 2013). Similar results were obtained for PEG-modified PLA-nanoparticles (Ishihara et al., 2009). The differences in the types of PEG polymer, physicochemical properties of liposomes (including particle size and Zeta potential), the animal species, encapsulated drug as well as dose of PEG-L may affect the time interval for inducing the ABC phenomenon. For instance, Ishida et al. (2004) reported the physicochemical properties of the first injected PEG-L (composed of HEPC, chol, and mPEG2000-DSPE) strongly affect the extent of the ABC phenomenon, which was greatly induced with 10 days interval between injections in their study. Saadati et al. (2013) illustrated the mass ratio of PLGA-PEG to etoposide was 6: 1 and the particle size of etoposide loaded PLGA-PEG was 173 nm, which were very different from our formulation. In this study, a dose of 0.05 μmoL/kg of PEG-B-L was pre-administered intravenously to five groups of rats for the first step. The subsequent doses of PEG-DTX-L were injected to each group after 0, 1, 3, 5, and 7 days. The results showed that a 3-day interval between doses triggered the strongest ABC phenomenon, and

then the magnitude gradually attenuated to a low extent in 7 days (Figure 1). Furthermore, the prolongation of time interval between doses could significantly alleviate the ABC magnitude (Table 3). Herein, the ABC phenomenon might be attenuated and even eliminated when the time interval was long enough.

However, the underlying mechanism of time interval-dependent ABC phenomenon has yet to be understood. This phenomenon is widely thought to be caused by an increased production of anti-PEG IgM secreted from the splenic B cells and subsequent complement activation, leading to the uptake of PEG-L by hepatic and splenic macrophage cells (Shimizu et al., 2015). Nevertheless, it still cannot clearly explain whether the presence of the anti-PEG IgM and complement is totally indispensable (Cui et al., 2008; Zhao et al., 2012), indicating that other factors may also be linked to the ABC phenomenon.

It is worth mentioning that the induction activity of hepatic CYPs is strongly influenced by acute exposure to xenobiotics, which can affect the metabolic process of co-medicated drugs by enhancing clearance of the victim drug (Riley and Wilson, 2015). However, whether CYPs are involved in the ABC phenomenon induced by repeated injection of PEG-L has not been verified. To clarify this issue, the relative activity of CYP isoforms were simultaneously determined by quantitative analysis of classical probe substrates of multiple CYPs based on a multiple-probe cocktail approach. In order to avoid potential interactions among the cocktail substrates, special care should be taken during the selection of the substrate concentrations in assessing CYP activity, and reducing the dosage of the substrate is one of the most effective methods. Based on previous studies and our preliminary experiments, the concentrations of probe substrates are 0.4 mg/kg except for amodiaquine (1.2 mg/kg) (Han et al., 2014; Sun et al., 2017). Because of the

inter-individual variation of CYP activity, sufficient number of subjects is required. Thereby, eight rats were used in each group for pharmacokinetic studies for assessing the activity of CYPs in the current study. Because male rats having 5 ~ 10-fold higher CYP3A activity than female rats and the level in male rats more closely matches the level in humans. Therefore, male rats were selected for *in vivo* experiments (Tomlinson et al., 1997; Bogaards et al., 2000). The activity of CYP3A1, CYP2C6 and CYP1A2 were significantly induced by repeated injection of PEG-L (with 3-day interval) in terms of altered pharmacokinetic parameters of corresponding probe substrates (Figure 2 and Supplemental Table 15~17), whereas the activity of CYP2B1, CYP2C7, CYP2C11 and CYP2D2 in the repeated PEG-L injection group were comparable to that of the control group (data no shown). Meanwhile, the highest mRNA and protein expression of CYP3A1, CYP2C6 and CYP1A2 were found in the repeated PEG-L injection group among the aforementioned five groups, and then gradually reduced with extended time intervals (Figure 3), which is in accordance with the magnitude of the ABC phenomenon (Table 3). Accordingly, it appears that the increased activity and expression of CYPs may have possible involvement in the induction of ABC phenomenon, which was confirmed by an inhibition study of the ABC phenomenon in the presence of CYP inhibitors**.** From the change of $AUC_{C/T}$ and $t_{1/2C/T}$ values, the ABC magnitude was slightly suppressed by KTZ pretreatment not by CIM, and the mRNA and protein of rat CYP3A1 and CYP1A2 were also significantly inhibited (Figure 5). Notably, when rats were pretreated with KTZ, the relative concentration of DTX in liver was more than threefold of rats that without KTZ pretreatment, while the DTX accumulation in spleen was not altered markedly (Figure 4B). By contrast, the ABC magnitude as well as DTX accumulation in liver and spleen was not affected by the prior administration of CIM (Figure 4D), indicating a negligible role of

CYP2C6 in the ABC phenomenon. These observations may be attributed to the fact that DTX is known to be mainly metabolized by CYP3A1/2, whose activity can be strongly inhibited by KTZ (Kotegawa et al., 2002). Thus, pretreatment with KTZ could suppress the oxidative metabolism of DTX from PEG-DTX-L in plasma and liver, leading to the response of the ABC magnitude of PEG-DTX-L to CYP3A1 inhibition. In this context, CYP3A1 may be involved in the induction of the ABC phenomenon. Consistent with the work presented in this study, the chemotherapeutic agents topotecan and etoposide are substrates of CYP3A1 and accelerated blood clearance of PEGylated liposomal topotecan and PEGylated PLGA etoposide followed by repeated injections have also been reported (Li et al., 2012; Najar et al., 2011; Skirvin et al., 2002; Saadati et al., 2013). In contrast, doxorubicin is primarily metabolized to doxorubicinol by cytoplasmic aldo-keto and carbonyl reductases, which may explain that the ABC phenomenon has never been observed for PEGylated liposomal doxorubicin (Robert and Gianni, 1993; Ishida et al., 2006a).

The ABC phenomenon was not abolished with the addition of CYP selective inhibitors. Apart from CYPs induction and anti-PEG IgM, a number of other factors might contribute to the ABC phenomenon, including the protein corona and lipoprotein receptor. Recently, it is reported that the protein corona (mainly consists of complement proteins and apolipoproteins with or without immunoglobulins) formed on polymer nanoparticles including PEG-L plays a predominant role in the clearance of the liposomes from the blood (Pozzi et al., 2014; Papi et al., 2017). In addition, it has been demonstrated that serum albumin and apolipoproteins low-density-lipoprotein receptor also have a positive impact on this phenomenon (Bertrand et al., 2017; Kari et al., 2017).

The present study has several limitations. Firstly, the CYP activity were investigated by evaluating the original probe substrates rather than their metabolites, and it would better to illustrate

the involvement of specific CYP isoform to see a corresponding increase in metabolite generation. Secondly, although the mRNA and protein of rat CYP1A2 were significantly inhibited by CIM (Figure 5C and D), it is yet to be confirmed whether the activity of CYP1A2 was also inhibited, a selective inhibitor of CYP1A2 is therefore needed to elucidate it. Surely, more strict experiments are needed to carry out for unveiling the underlying mechanisms, such as CYP3A knockout mouse or transgenic mouse model expressing CYP3A which might give much straight evidence.

Taken together, in light of the data obtained with pharmacokinetics and biodistribution as well as mRNA and protein of rat CYPs, this is the first observation that the increased activity and expression of CYP3A1 may be involved in the induction of the ABC phenomenon. However, the relative contribution of CYPs in the induction process of the ABC phenomenon remains unknown. Is there a relationship or crosstalk among CYPs and other factors in the induction of the ABC phenomenon? It is therefore particularly interesting to understand how PEG-L affect the biological fate of these clinically relevant CYPs.

Acknowledgements

The authors thank all the members from Center for Drug Delivery Systems, Shanghai Institute of Materia Medica, Chinese Academy of Sciences for their technical assistance and support in LC-MS/MS.

Author contributions

Participated in research design: Daiyin Peng, Weidong Chen, Jiwen Zhang, and Fengling Wang. **Conducted experiments:** Fengling Wang, Yifan Wu, Huihui Wang, and Xiaoting Xie. **Validation and Performed data analysis:** Jiwen Zhang, Yifan Wu, Huihui Wang, and Xi Ye. **Wrote/contributed to the writing of the manuscript:** Fengling Wang, and Weidong Chen.

References

Bansal S and DeStefano A (2007) Key elements of bioanalytical method validation for small molecules. *AAPS J* **9:**E109-114.

Bertrand N, Grenier P, Mahmoudi M, Lima E, Appel E, Dormont F, Lim J, Karnik R, Langer R, and Farokhzad O (2017) Mechanistic understanding of in vivo protein corona formation on polymeric nanoparticles and impact on pharmacokinetics. *Nat Commun* **8:**777.

Bogaards J, Bertrand M, Jackson P, Oudshoorn M, Weaver R, van Bladeren P, and Walther B (2000) Determining the best animal model for human cytochrome P450 activities: a comparison of mouse, rat, rabbit, dog, micropig, monkey and man. *Xenobiotica* **30:**1131-1152.

Burkina V, Rasmussen M, Pilipenko N, and Zamaratskaia G (2017) Comparison of xenobiotic-metabolising human, porcine, rodent, and piscine cytochrome P450. *Toxicology* **375:**10-27.

Cui J, Li C, Wang C, Li Y, Zhang L, Zhang L, and Yang H (2008) Repeated injection of pegylated liposomal antitumour drugs induces the disappearance of the rapid distribution phase. *J Pharm Pharmacol* **60:**1651-1657.

Dams E, Laverman P, Oyen W, Storm G, Scherphof G, van Der Meer J, Corstens F, and Boerman O (2000) Accelerated blood clearance and altered biodistribution of repeated injections of sterically stabilized liposomes. *J Pharmacol Exp Ther* **292:**1071-1079.

Doak S and Zaŕ Z (2012) Real-time reverse-transcription polymerase chain reaction: technical considerations for gene expression analysis. *Methods Mol Biol* **817:**251-270.

Gabizon A, Shmeeda H, and Barenholz Y (2003) Pharmacokinetics of pegylated liposomal Doxorubicin: review of animal and human studies. *Clin Pharmacokinet* **42:**419-436.

Gai X, Cheng L, Li T, Liu D, Wang Y, Wang T, Pan W, and Yang X (2018) In vitro and In vivo Studies on a Novel Bioadhesive Colloidal System: Cationic Liposomes of Ibuprofen. *AAPS PharmSciTech* **19:**700-709.

Guengerich F (2008) Cytochrome p450 and chemical toxicology. *Chem Res Toxicol* **21:**70-83.

Han Y, Li D, Yang Q, Zhou Z, Liu L, Li B, Lu J, and Guo C (2014) In vitro inhibitory effects of scutellarin on six human/rat cytochrome P450 enzymes and P-glycoprotein. *Molecules* **19:**5748-5760.

He R, Ye X, Li R, Chen W, Ge T, Huang T, Nie X, Chen H, Peng D, and Chen W (2017) PEGylated niosomes-mediated drug delivery systems for Paeonol: preparation, pharmacokinetics studies and synergistic anti-tumor effects with 5-FU. *J Liposome Res* **27:**161-170.

Huang X, Chen Y, Peng D, Li Q, Wang X, Wang D, and Chen W (2013) Solid lipid nanoparticles as delivery systems for Gambogenic acid. *Colloids Surf B Biointerfaces* **102:**391-397.

Immordino M, Dosio F, and Cattel L (2006) Stealth liposomes: review of the basic science, rationale, and clinical applications, existing and potential. *Int J Nanomedicine* **1:**297-315.

Ingelman-Sundberg M (2004) Pharmacogenetics of cytochrome P450 and its applications in drug therapy: the past, present and future. *Trends Pharmacol Sci* **25:**193-200.

Ishida T, Atobe K, Wang X, and Kiwada H (2006a) Accelerated blood clearance of PEG-L upon repeated injections: effect of doxorubicin-encapsulation and high-dose first injection. *J Control Release* **115:**251-258.

Ishida T, Harada M, Wang X, Ichihara M, Irimura K, and Kiwada H (2005) Accelerated blood clearance of PEG-L following preceding liposome injection: effects of lipid dose and PEG

surface-density and chain length of the first-dose liposomes. *J Control Release* **105:**305-317.

Ishida T, Ichihara M, Wang X, and Kiwada H (2006b) Spleen plays an important role in the induction of accelerated blood clearance of PEG-L. *J Control Release* **115:**243-250.

Ishida T, Ichihara M, Wang X, Yamamoto K, Kimura J, Majima E, and Kiwada H (2006c) Injection of PEG-L in rats elicits PEG-specific IgM, which is responsible for rapid elimination of a second dose of PEG-L. *J Control Release* **112:**15-25.

Ishida T, Ichikawa T, Ichihara M, Sadzuka Y, and Kiwada H (2004) Effect of the physicochemical properties of initially injected liposomes on the clearance of subsequently injected PEG-L in mice. *J Control Release* **95:**403-412.

Ishida T, Kashima S, and Kiwada H (2008) The contribution of phagocytic activity of liver macrophages to the accelerated blood clearance (ABC) phenomenon of PEG-L in rats. *J Control Release* **126:**162-165.

Ishida T, Maeda R, Ichihara M, Irimura K, and Kiwada H (2003) Accelerated clearance of PEG-L in rats after repeated injections. *J Control Release* **88:**35-42.

Ishihara T, Takeda M, Sakamoto H, Kimoto A, Kobayashi C, Takasaki N, Yuki K, Tanaka K, Takenaga M, Igarashi R, Maeda T, Yamakawa N, Okamoto Y, Otsuka M, Ishida T, Kiwada H, Mizushima Y, and Mizushima T (2009) Accelerated blood clearance phenomenon upon repeated injection of PEG-modified PLA-nanoparticles. *Pharm Res* **26:**2270-2279.

Kari O, Rojalin T, Salmaso S, Barattin M, Jarva H, Meri S, Yliperttula M, Viitala T, and Urtti A (2017) Multi-parametric surface plasmon resonance platform for studying liposome-serum interactions and protein corona formation. *Drug Deliv Transl Res* **7:**228-240.

Koide H, Asai T, Hatanaka K, Akai S, Ishii T, Kenjo E, Ishida T, Kiwada H, Tsukada H, and Oku

N (2010) T cell-independent B cell response is responsible for ABC phenomenon induced by repeated injection of PEG-L. *Int J Pharm* **392:**218-223.

Koide H, Asai T, Kato H, Ando H, Shiraishi K, Yokoyama M, and Oku N (2012) Size-dependent induction of accelerated blood clearance phenomenon by repeated injections of polymeric micelles. *Int J Pharm* **432:**75-79.

Kotegawa T, Laurijssens B, Von Moltke L, Cotreau M, Perloff M, Venkatakrishnan K, Warrington J, Granda B, Harmatz J, and Greenblatt D (2002) In vitro, pharmacokinetic, and pharmacodynamic interactions of ketoconazole and midazolam in the rat. *J Pharmacol Exp Ther* **302:**1228-1237.

Laginha K, Verwoert S, Charrois G, and Allen T (2005) Determination of doxorubicin levels in whole tumor and tumor nuclei in murine breast cancer tumors. *Clin Cancer Res* **11:**6944-6949.

Lee B, Ji H, Lee T, and Liu K (2015) Simultaneous screening of activities of five cytochrome P450 and four uridine 5'-diphospho-glucuronosyltransferase enzymes in human liver microsomes using cocktail incubation and liquid chromatography-tandem mass spectrometry. *Drug Metab Dispos* **43:**1137-1146.

Levine M, Law EY, Bandiera SM, Chang TK, and Bellward GD (1998) In vivo cimetidine inhibits hepatic CYP2C6 and CYP2C11 but not CYP1A1 in adult male rats. *J Pharmacol Exp Ther* **284:**493-499.

Lewis D, Ioannides C, and Parke D (1998) Cytochromes P450 and species differences in xenobiotic metabolism and activation of carcinogen. *Environ Health Perspect* **106:**633-641.

Li C, Cao J, Wang Y, Zhao X, Deng C, Wei N, Yang J, and Cui J (2012) Accelerated blood clearance of pegylated liposomal topotecan: influence of polyethylene glycol grafting density

and animal species. *J Pharm Sci* **101:**3864-3876.

Li C, Zhao X, Wang Y, Yang H, Li H, Li H, Tian W, Yang J, and Cui J (2013) Prolongation of time interval between doses could eliminate accelerated blood clearance phenomenon induced by pegylated liposomal topotecan. *Int J Pharm* **443:**17-25.

Lin J and Lu A (1998) Inhibition and induction of cytochrome P450 and the clinical implications. *Clin Pharmacokinet* **35:**361-390.

Lu C and Li A (2001) Species comparison in P450 induction: effects of dexamethasone, omeprazole, and rifampin on P450 isoforms 1A and 3A in primary cultured hepatocytes from man, Sprague-Dawley rat, minipig, and beagle dog. *Chem Biol Interact* **134:**271-281.

Ma Y, Yang Q, Wang L, Zhou X, Zhao Y, and Deng Y (2012) Repeated injections of PEGylated liposomal topotecan induces accelerated blood clearance phenomenon in rats. *Eur J Pharm Sci* **45:**539-545.

Meredith C, Maldonado A, and Speeg K (1985) The effect of ketoconazole on hepatic oxidative drug metabolism in the rat in vivo and in vitro. *Drug Metab Dispos* **13:**156-162.

Mosca P, Bonazzi P, Novelli G, Jezequel A, and Orlandi F (1985) In vivo and in vitro inhibition of hepatic microsomal drug metabolism by ketoconazole. *Br J Exp Pathol* **66:**737-742.

Najar IA, Sharma SC, Singh GD, Koul S, Gupta PN, Javed S and Johri RK (2011) Involvement of P-glycoprotein and CYP 3A4 in the enhancement of etoposide bioavailability by a piperine analogue. *Chem Biol Interact* **190**: 84-90.

Nishiya Y, Hagihara K, Ito T, Tajima M, Miura S, Kurihara A, Farid N, and Ikeda T (2009) Mechanism-based inhibition of human cytochrome P450 2B6 by ticlopidine, clopidogrel, and the thiolactone metabolite of prasugrel. *Drug Metab Dispos* **37:**589-593.

Papi M, Caputo D, Palmieri V, Coppola R, Palchetti S, Bugli F, Martini C, Digiacomo L, Pozzi D, and Caracciolo G (2017) Clinically approved PEGylated nanoparticles are covered by a protein corona that boosts the uptake by cancer cells. *Nanoscale* **9:**10327-10334.

Pozzi D, Colapicchioni V, Caracciolo G, Piovesana S, Capriotti AL, Palchetti S, De Grossi S, Riccioli A, Amenitsch H, and Laganà A (2014) Effect of polyethyleneglycol (PEG) chain length on the bio–nano-interactions between PEGylated lipid nanoparticles and biological fluids: from nanostructure to uptake in cancer cells. *Nanoscale* **6:**2782-2792.

Riley R and Wilson C (2015) Cytochrome P450 time-dependent inhibition and induction: advances in assays, risk analysis and modelling. *Expert Opin Drug Metab Toxicol* **11:**557-572.

Rio D, Ares M, Hannon G, and Nilsen T (2010) Purification of RNA using TRIzol (TRI reagent). *Cold Spring Harb Protoc* **2010:**pdb.prot5439.

Robert J and Gianni L (1993) Pharmacokinetics and metabolism of anthracyclines. *Cancer Surv* **17**:219-252.

Roth R, Madhani H, and Garcia J (2018) Total RNA Isolation and Quantification of Specific RNAs in Fission Yeast. *Methods Mol Biol* **1721:**63-72.

Saadati R, Dadashzadeh S, Abbasian Z, and Soleimanjahi H (2013) Accelerated blood clearance of PEGylated PLGA nanoparticles following repeated injections: effects of polymer dose, PEG coating, and encapsulated anticancer drug. *Pharm Res* **30:**985-995.

Shimizu T, Mima Y, Hashimoto Y, Ukawa M, Ando H, Kiwada H, and Ishida T (2015) Anti-PEG IgM and complement system are required for the association of second doses of PEG-L with splenic marginal zone B cells. *Immunobiology* **220:**1151-1160.

Skirvin JA and Lichtman SM (2002) Pharmacokinetic considerations of oral chemotherapy in

elderly patients with cancer. *Drugs Aging* **19**:25-42.

Suk J, Xu Q, Kim N, Hanes J, and Ensign L (2016) PEGylation as a strategy for improving nanoparticle-based drug and gene delivery. *Adv Drug Deliv Rev* **99:**28-51.

Sun J, Lu Y, Li Y, Pan J, Liu C, Gong Z, Huang J, Zheng J, Zheng L, Li Y, Liu T, and Wang Y (2017) Influence of shenxiong glucose injection on the activities of six CYP isozymes and metabolism of warfarin in rats assessed using probe cocktail andpharmacokinetic approaches. *Molecules* **22**.

Suzuki T, Ichihara M, Hyodo K, Yamamoto E, Ishida T, Kiwada H, Kikuchi H, and Ishihara H (2014) Influence of dose and animal species on accelerated blood clearance of PEGylated liposomal doxorubicin. *Int J Pharm* **476:**205-212.

Tomlinson E, Maggs J, Park B, and Back D (1997) Dexamethasone metabolism in vitro: species differences. *J Steroid Biochem Mol Biol* **62:**345-352.

Tracy T, Chaudhry A, Prasad B, Thummel K, Schuetz E, Zhong X, Tien Y, Jeong H, Pan X, Shireman L, Tay-Sontheimer J, and Lin Y (2016) Interindividual Variability in Cytochrome P450-Mediated Drug Metabolism. *Drug Metab Dispos* **44:**343-351.

Turpeinen M, Hofmann U, Klein K, Mürdter T, Schwab M, and Zanger UM (2009) A predominate role of CYP1A2 for the metabolism of nabumetone to the active metabolite, 6-Methoxy-2-naphthylacetic acid, in human liver microsomes. *Drug Metabolism and Disposition* **37:**1017.

Uoto K, Mitsui I, Terasawa H, and Soga T (1997) First synthesis and cytotoxic activity of novel docetaxel analogs modified at the C18-position. *Bioorganic & Medicinal Chemistry Letters* **7:**2991-2996.

US FDA (2017a) Guidance for Industry: Clinical drug interaction studies -study design, data analysis, and clinical implications. draft guidance. Available at: https://www.fda.gov/downloads/drugs/guidancecomplianceregulatoryinformation/guidances/ucm292362.pdf

US FDA (2017b) Drug development and drug interactions: table of substrates, inhibitors and inducers. https://www.fda.gov/drugs/developmentapprovalprocess/developmentresources/druginteractionslabeling/ucm093664.htm#table3-2

US FDA (2018) Department of Health and Human Services Center for Drug Evaluation and Research (CDER), Center for Veterinary Medicine (CVM). Guidance for industry: bioanalytical method validation. https://www.fda.gov/downloads/drugs/ guidance compliance regulatory information/guidances/ucm070107.pdf.

Vaclavikova R, Soucek P, Svobodova L, Anzenbacher P, Simek P, Guengerich F, and Gut I (2004) Different in vitro metabolism of paclitaxel and docetaxel in humans, rats, pigs, and minipigs. *Drug Metab Dispos* **32:**666-674.

Veronese F and Pasut G (2005) PEGylation, successful approach to drug delivery. *Drug Discov Today* **10:**1451-1458.

Walsky R and Obach R (2004) Validated assays for human cytochrome P450 activities. *Drug Metab Dispos* **32:**647-660.

Wang X, Han A, Wen C, Chen M, Chen X, Yang X, Ma J, and Lin G (2013) The effects of H2S on the activities of CYP2B6, CYP2D6, CYP3A4, CYP2C19 and CYP2C9 in vivo in rat. *Int J Mol Sci* **14:**24055-24063.

Xu H, Ye F, Hu M, Yin P, Zhang W, Li Y, Yu X, and Deng Y (2015) Influence of phospholipid types and animal models on the accelerated blood clearance phenomenon of PEG-L upon repeated injection. *Drug Deliv* **22:**598-607.

Yang L, Yan C, Zhang F, Jiang B, Gao S, Liang Y, Huang L, and Chen W (2018) Effects of ketoconazole on cyclophosphamide metabolism: evaluation of CYP3A4 inhibition effect using the in vitro and in vivo models. *Exp Anim* **67:**71-82.

Yang Q, Ma Y, Zhao Y, She Z, Wang L, Li J, Wang C, and Deng Y (2013) Accelerated drug release and clearance of PEGylated epirubicin liposomes following repeated injections: a new challenge for sequential low-dose chemotherapy. *Int J Nanomedicine* **8:**1257-1268.

Zhao Y, Wang C, Wang L, Yang Q, Tang W, She Z, and Deng Y (2012) A frustrating problem: accelerated blood clearance of PEGylated solid lipid nanoparticles following subcutaneous injection in rats. *Eur J Pharm Biopharm* **81:**506-513.

Footnotes

This work was supported by the National Natural Science Foundation of China (NO. 81773988) and Natural Science Foundation of Anhui University of Chinese Medicine (2018zrzd04).

Legends for Figures

Figure 1. Effect of repeated injection time interval on the magnitude of the ABC phenomenon. (A) The mean concentration-time (0 ~ 12 hr) profile of DTX in rats after a single or repeated injection of PEG-L. The relative concentration represents the relative ratio with the initial concentration (at 0.167 hr) of control. (B) Liver and spleen distribution (12 hr) of DTX in rats after the second injection of PEG-DTX-L. The relative concentration represents the relative ratio with the liver and spleen concentration of control, respectively. Rats in five groups (1 d, 3 d, 5 d and 7 d) were injected with two injections of PEG-L with various time intervals (1 day, 3 days, 5 days and 7 days, respectively). Group 0 d represents a single dose of PEG-L, which is a control for other test groups. $^{*}P < 0.05$, $^{**}P < 0.01$ compared with control (0 d) (n=6, mean ± SD).

Figure 2. Effect of a single injection or repeated injection of PEG-L on the pharmacokinetic profiles of midazolam, diclofenac and phenacetin in rats. (A) The mean concentration-time (0 ~ 360 min) profile of midazolam (probe for CYP3A1) in rats after the second injection of PEG-L. The relative concentration represents the relative ratio with the initial concentration (at 3 min) of single PEG-L injection equal to 100%. The impact of repeated PEG-L injection on the plasma concentrations of the CYP2C6 substrate diclofenac and the CYP1A2 substrate phenacetin are presented in panel B and C, respectively. As described in table 2, animals in single PEG-L injection group received a single PEG-L injection followed by intravenous injection of probe cocktail solution after 30 min. In the repeated PEG-L injection group, animals received the initial

PEG-L injection and a second injection 3 days later followed by intravenous injection of probe cocktail solution after 30 min. Data are presented as the mean ± SD (n=8).

Figure 3. Effect of single or repeated injection of PEG-L on the mRNA and protein expression of hepatic CYPs. The CYPs expression profiles were determined after the first injection of PEG-L followed by a subsequent injection of PEG-DTX-L at different time intervals. The normal control group (NC) was injected with the same volume PBS as a single injection. After 1, 3, 5, and 7 days (1 d, 3 d, 5 d, and 7 d), the liver was isolated as described in materials and methods. (A) RT-qPCR analysis detected the relative mRNA expression of CYP3A1, CYP2C6 and CYP1A2 in liver. Values were normalized to the respective control groups and fold change was calculated by $2^{-\Delta\Delta CT}$ method using β-actin as an endogenous reference gene. (B) Western blot analysis measured the relative protein expression levels of CYP3A1, CYP2C6 and CYP1A2 in liver. Bar graphs show quantitative evaluation of CYP3A1, CYP2C6 and CYP1A2 bands by densitometry from triplicate independent experiments. Each band density was evaluated by ImageJ software and these data were evaluated as percentage compared to GAPDH. 0 d indicates the group received only a single injection of PEG-DTX-L. 1 d, 3 d, 5 d and 7 d indicate these groups received two injections of PEG-L at different time intervals (1 day, 3 days, 5 days and 7 days, respectively). Data are presented as the mean ± SD (n=5 ~ 6). $^{*}P < 0.05$, $^{**}P < 0.01$ compared with 0 d group. NC, normal control group.

Figure 4. Effects of CYP inhibitors on the magnitude of the ABC phenomenon. (A) The mean concentration-time (0 ~ 12 hr) profile of DTX in rats after the second injection of PEG-DTX-L pretreated with CYP inhibitors. The relative concentration represents the relative ratio with the initial concentration (at 10 min) of control. (B) Liver and spleen distribution (12 hr) of DTX in

rats after the second injection of PEG-DTX-L. The relative concentration represents the relative liver and spleen concentration of control versus KTZ and CIM treated groups. For A and B, 3 d KTZ+ rats were pre-gavaged with KTZ (100 mg/kg/day) for 7 days and treated with the repeated PEG- L injection afterwards; 3 d KTZ- rats were pretreated with an equal volume vehicle for 7 days and then treated with the repeated PEG- L injection; Control rats were pretreated with an equal volume vehicle for 7 days followed by a single PEG-L injection. For C and D, 3 d CIM+ rats received the first PEG-L injection, and 3 days later, rats were pretreated with a single dose (150 mg/kg) of CIM for 1.5 hr before the second PEG-L dose; 3 d CIM- rats received the first PEG-L injection, and 3 days later, rats were pretreated with an equal volume vehicle for 1.5 hr before the repeated PEG-L injection; Control rats were pretreated with an equal volume vehicle for 1.5 hr followed by a single PEG-L injection. $^{*}P < 0.05$, $^{**}P < 0.01$ compared with control; $^{\#\#}P < 0.01$ compared with 3 d (KTZ-) (n=6, mean ± SD). KTZ, ketoconazole; CIM, cimetidine.

Figure 5. Effects of the presence of CYP inhibitors on mRNA and protein expression of CYPs. By pretreated with control vehicle or enzyme inhibitors before administration of repeated PEG-L injection with a time interval of 3 days, the respective expression levels of hepatic CYPs were determined. (A) RT-qPCR analysis detected the relative mRNA expression levels of hepatic CYP3A1, CYP2C6 and CYP1A2 in the presence of the CYP3A1 inhibitor, KTZ or the CYP2C6 inhibitor, CIM (C). Values were normalized to the respective control groups and fold change was calculated by $2^{-\Delta\Delta CT}$ method using β-actin as an endogenous reference gene. (B) Western blot analysis measured the relative protein expression levels of hepatic CYP3A1, CYP2C6 and CYP1A2 in the presence of the CYP3A1 inhibitor, KTZ or the CYP2C6 inhibitor, CIM (D). Bar graphs show quantitative evaluation of CYP3A1, CYP2C6 and CYP1A2 bands by densitometry

from triplicate independent experiments. Each band density was evaluated by ImageJ software and these data were evaluated as percentage compared to GAPDH. In group 0 d, animals received a single injection of PEG-L and intravenous injection of probe cocktail solution after 30 min. Data are presented as the mean ± SD (n=5 ~ 6). $^{*}P < 0.05$, $^{**}P < 0.01$ compared with 0 d group; $^{\#}P < 0.05$, $^{\#\#}P < 0.01$ compared with 3 d (KTZ-) or 3 d (CIM-). KTZ, ketoconazole; CIM, cimetidine.

DMD Fast Forward. Published on January 23, 2019 as DOI: 10.1124/dmd.118.085340
This article has not been copyedited and formatted. The final version may differ from this version.

Tables

Table 1 Injection protocols for PEG-B-L and PEG-DTX-L

Factor	Group	First injection liposomes	Time interval (day)	Second injection (2.5 mg/kg)
Time interval	0 d	PEG-DTX-L (2.50 mg/kg, containing 0.05 μmoL of PEG-DSPE/kg)	0	None
	1 d	PEG-B-L (0.05 μmoL of PEG-DSPE/kg)	1	PEG- DTX-L
	3 d		3	PEG- DTX-L
	5 d		5	PEG- DTX-L
	7 d		7	PEG- DTX-L

0 d indicates the group received only a single injection of PEG-DTX-L. 1 d, 3 d, 5 d and 7 d indicate these groups received two injections of PEG-L at different time intervals (1 day, 3 days, 5 days and 7 days, respectively). Abbreviation: PBS, phosphate buffer saline; PEG-DTX-L, PEGylated liposomal docetaxel; PEG-B-L, blank PEGylated liposomes.

Table 2 Injection protocols for cocktail probes

Group	First injection	Time interval (days)	Second injection (2.5 mg/kg) + cocktail probes (1.0 mg/kg)
Control	PBS	3	PBS + Cocktail probes
Single DTX injection	DTX injection (2.5 mg/kg)	0	Cocktail probes
Repeated DTX injection	DTX injection (2.5 mg/kg)	3	DTX injection + Cocktail probes
Single PEG-L injection	PEG-DTX-L (2.5 mg/kg)	0	Cocktail probes
Repeated PEG-L injection	PEG-B-L	3	PEG-DTX-L + Cocktail probes

0 d indicates these groups received only a single injection of DTX injection or PEG-DTX-L. 3 d, indicate these groups received repeated injection of DTX injection or PEG-L with a 3-day interval.

Abbreviation: PBS, phosphate buffer saline; PEG-L, PEGylated liposomes; PEG-DTX-L, PEGylated liposomal docetaxel; PEG-B-L, blank PEGylated liposomes.

Table 3 Pharmacokinetic parameter ratios for the magnitude of the ABC phenomenon

(mean ± SD, n = 6)

Parameter	Control	Repeated injection group			
		1 d	3 d	5 d	7 d
$^{\triangle}AUC_{C/T}$	1.00	1.62±0.17	3.14±0.59	2.44±0.31	1.70±0.19
$^{\triangle}t_{1/2C/T}$	1.00	1.38±0.23	2.54±0.24	1.62±0.20	1.50±0.12

AUC_{0-t}, area under curve from time 0 to t; $t_{1/2}$, half-life; d, day. $^{\triangle}$Represents a pharmacokinetic parameter ratio of the control group to the test group.

DMD Fast Forward. Published on January 23, 2019 as DOI: 10.1124/dmd.118.085340
This article has not been copyedited and formatted. The final version may differ from this version.

Figures

Figure 1

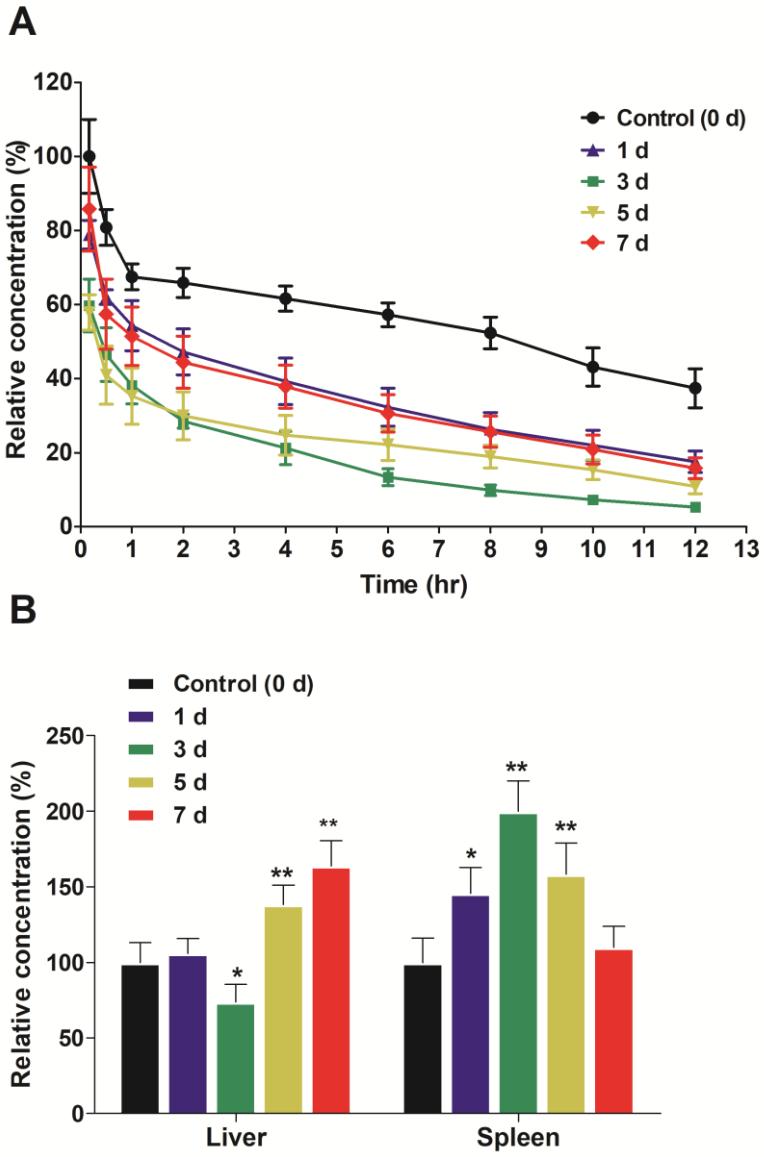

DMD Fast Forward. Published on January 23, 2019 as DOI: 10.1124/dmd.118.085340
This article has not been copyedited and formatted. The final version may differ from this version.

Figure 2

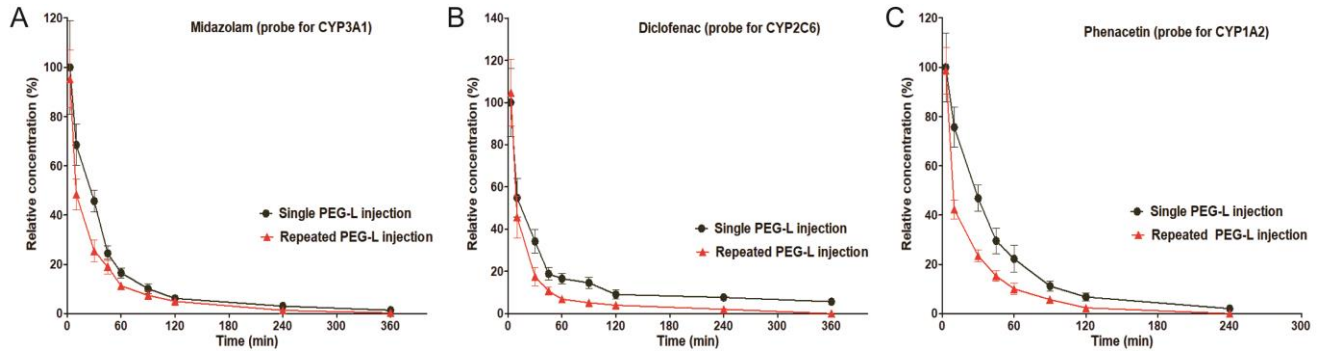

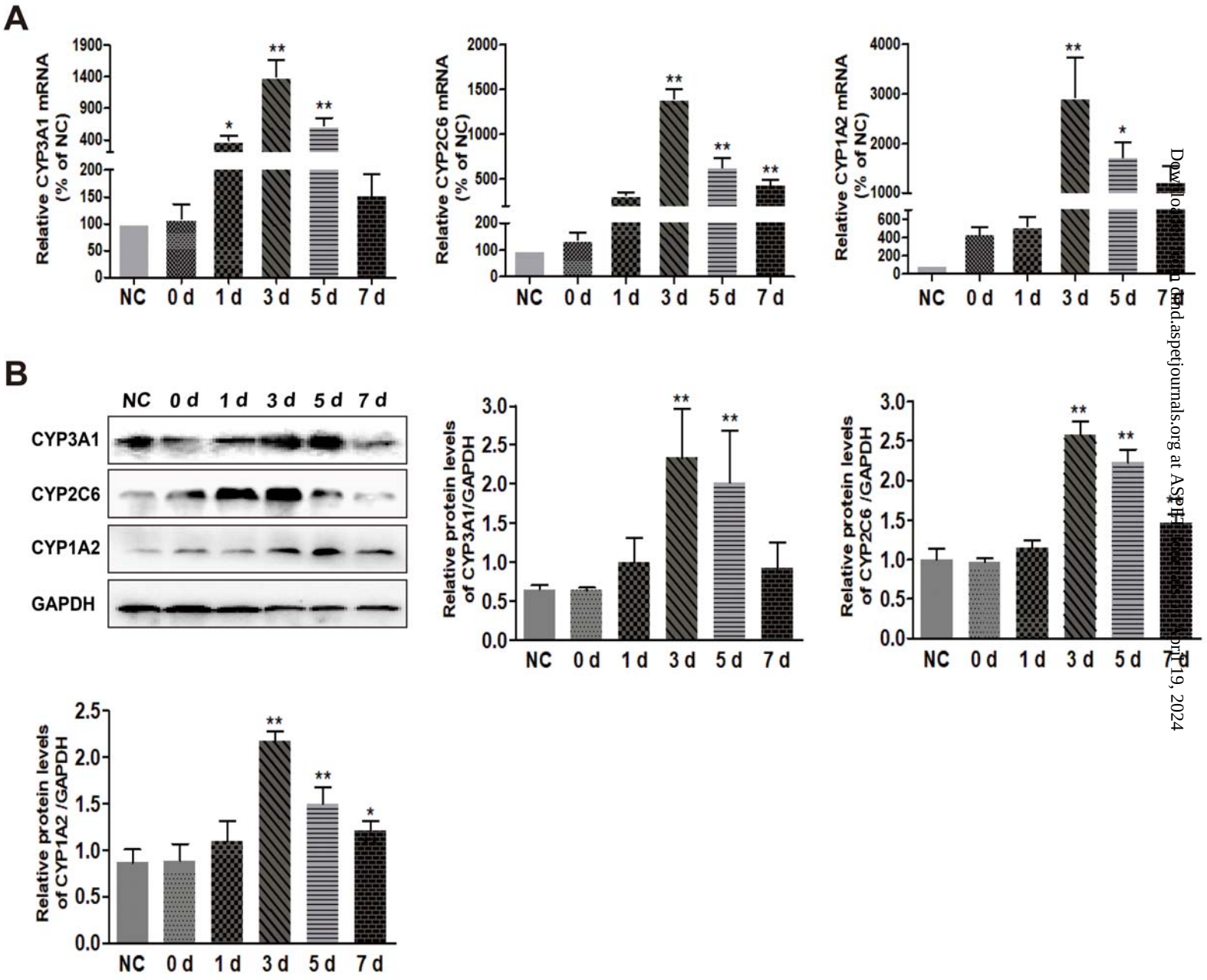

DMD Fast Forward. Published on January 23, 2019 as DOI: 10.1124/dmd.118.085340
This article has not been copyedited and formatted. The final version may differ from this version.

Figure 4